The spatial, temporal and contrast properties of expansion and rotation flight optomotor responses in *Drosophila*

Brian J. Duistermars, Dawnis M. Chow, Michael Condro and Mark A. Frye*

Department of Physiological Science, University of California, Los Angeles, CA 90095-1606, USA

*Author for correspondence (e-mail: frye@physci.ucla.edu)

Summary

Fruit flies respond to panoramic retinal patterns of visual expansion with robust steering maneuvers directed away from the focus of expansion to avoid collisions and maintain an upwind flight posture. Panoramic rotation elicits comparatively weak syndirectional steering maneuvers, which also maintain visual stability. Full-field optic flow patterns like expansion and rotation are elicited by distinct flight maneuvers such as body translation during straight flight or body rotation during hovering, respectively. Recent analyses suggest that under some experimental conditions the rotation optomotor response reflects the linear sum of different expansion response components. Are expansion and rotation-mediated visual stabilization responses part of a single optomotor response subserved by a neural circuit that is differentially stimulated by the two flow fields, or rather do the two behavioral responses reflect two distinct control systems? Guided by the principle that the properties of neural circuits are revealed in the behaviors they mediate, we systematically varied the spatial, temporal and contrast properties of expansion and rotation stimuli, and quantified the time course and amplitude of optomotor responses during tethered flight. Our results support the conclusion that expansion and rotation optomotor responses are indeed two separate reflexes, which draw from the same system of elementary motion detectors, but are likely mediated by separate pre-motor circuits having different spatial integration properties, low-pass characteristics and contrast sensitivity.

Key words vision, optic flow, insect flight, motor control, wing kinematics.

Introduction

The sense of sight is crucial for navigating object-cluttered landscapes. For many creatures, including humans, visual cues are used to stabilize gaze on particular objects of interest, to stabilize head movements against body movements, and to estimate motion generated during locomotion (for a review, see Zanker and Zeil, 2001). Gaze stabilization results in a moving visual panorama being actively fixed on the retina by compensatory head or eye movements. The input to gaze stabilization, the retinal movement patterns termed optic flow, is highly complex and contains cues generated by forward translation as well as rotation. There is some evidence that the brain processes these two flow fields independently (Sandini et al., 2001; Dahmen et al., 2001). Indeed, the optic flow fields generated by translation and rotation are very different, with the first resembling diverging and converging lines of longitude on a globe, and the latter resembling parallel lines of latitude. We still have a relatively poor understanding of how these flow fields are processed and transformed into appropriate gaze stabilizing motor commands.

For flying insects, experimental rotation of the visual panorama results in the animal actively turning in the direction of motion. This robust behavioral attempt to minimize retinal slip comprises a classical 'optomotor' response thought to help maintain stability in the face of external perturbations such as a gust of wind, or internal perturbations such as bilaterally asymmetric motor output (Collett, 1980; Götz and Wandel, 1984; Götz, 1964; Heisenberg and Wolf, 1984). Behavioral optomotor responses, as well as their electrophysiological correlates within motion processing interneurons in the brain, show distinct tuning curves for the spatial, temporal and contrast structure of moving images (Buchner, 1984; Götz, 1975; O'Carroll et al., 1996).

A recent study of optomotor responses in fruit flies explicitly compared optomotor responses to rotation and translation stimuli and reported that panoramic patterns of image expansion/contraction centered laterally (approximating a visual stimulus generated during a side-slip maneuver) triggered optomotor responses that were three times stronger than responses to a rotating panorama of identical spatial and temporal structure (Tammero et al., 2004). This increase in gain emerges because the directional optomotor response to motion restricted to the rear hemisphere is reversed compared to frontal hemisphere motion. Thus, counterclockwise motion across the front, coupled with clockwise motion across the rear, produces a strong counterclockwise steering response oriented away from the focus of expansion (centered at the animal's right side in this example). The time course and magnitude of full-field rotational optomotor responses are nearly identical to the arithmetic sum of half-field expansion responses. Are rotation

and expansion optomotor responses controlled by a single expansion-sensitive circuit that is sub-optimally stimulated by full-field rotation cues? Alternatively, are optomotor responses mediated by separate optomotor control systems tuned specifically for rotation and expansion cues, respectively?

In the present study we tested the hypothesis that the spatial, temporal and contrast sensitivity of optomotor responses vary for rotational *versus* translational flow fields, which would support the idea that these motor responses are indeed distinct and thus mediated by separate and parallel pre-motor visual processing pathways. Using a tethered flight simulator, we measured the time course and amplitude of yaw torque wing kinematics in response to systematic variation of spatial frequency, temporal frequency, vertical pattern size and contrast for optic flow fields that differ only in gross spatial organization. Our results show that spatial and temporal frequency sensitivity is similar for rotation and expansion optomotor responses, suggesting common elementary motion detection. However, impulse–response dynamics, spatial integration properties and contrast sensitivity vary markedly for the two stimulus types, suggesting that after the earliest stages of motion coding, the two patterns of optic flow are processed by separate and distinct control systems, most likely comprising separate neuronal circuitry.

Materials and methods

Animals and preparation

A *Drosophila melanogaster* colony was reared on standard medium under a 12 h:12 h L:D cycle. Female adult flies, 4–6 days post pupal eclosion, were selected for use in this study. Animals were cold-anesthesized and tethered to a 0.1 mm tungsten rod with UV-activated glue (Kemxert Corp., York, PA, USA). After at least 1 h of recovery, individual animals were placed within a custom-built computer-controlled electronic flight simulator composed of a cylindrical 96×32 array of green-light-emitting diodes (LEDs) spanning 330° in azimuth and ±60° in zenith, as seen by the animal (Fig. 1A). There was a gap directly behind the animal to accommodate the tether (Fig. 1A). This narrow open space is not seen by the front-facing animal, and so does not significantly influence the optomotor performance. Each pixel was independently addressable at eight grayscale levels at a maximum of 72 cd m^{-2}, and the periodic contrast was approximately 93%. Each individual LED subtended 3.75° on the retina, therefore pattern motion was approximated using apparent motion stimuli. Both the motion of the projected pattern and the spatial pattern itself could be instantaneously modified under computer control. The manufacture, control and spectral details of the LED display used here are detailed elsewhere (Reiser and Dickinson, in press).

The wing kinematics exhibited in response to optomotor stimuli were encoded by an optical wingbeat analyzer in which an infrared beam casts a shadow of each beating wing onto a photodiode pair (Fig. 1A). The two optical signals are conditioned such that sensor output represents time-varying wing position. Associated electronics then process the analog position signal to extract total wing beat amplitude (ΣWBA) for the left and right wings, as well as total wing stroke frequency for each individual stroke. The difference in amplitude between the left and right wings (ΔWBA) is directly proportional to yaw torque (Götz, 1987; Tammero et al., 2004), and the cubed product of total stroke amplitude and frequency is roughly proportional to the aerodynamic power output during flight (Dickinson et al., 1998). These values are digitized by a standard PC data acquisition system, and also relayed to control the velocity of the LED display under closed-loop conditions.

Visual motion stimuli, acquisition and data analysis

Apparent motion was generated by panoramic patterns of vertical stripes moving horizontally. We examined responses to two motion patterns. The first was a classical optomotor stimulus consisting of a rotating striped 'drum'. For this stimulus, the pattern simply rotated at constant velocity around the fly in a clockwise direction (viewed from above), therefore the velocity profile was constant along 360° of azimuth. The second stimulus was identical to the rotating drum except that the direction of motion in the rear visual hemisphere was reversed, forming a pseudo-translation flow field. This pattern of image motion produced a focus of expansion centered 90° to the left of the animal, and a focus of contraction 90° to the right. In other words, the pattern expanded from the left and contracted to the right of the fly (Fig. 1B). The azimuthal velocity profile follows a square-wave trajectory rather than following a smooth sinusoidal trajectory. This stimulus produces strong motion cues near the poles of expansion and contraction, and we therefore refer to this stimulus as an 'expansion' cue. This large-field visual expansion stimulus elicits robust steering responses in *Drosophila* (Tammero et al., 2004). During flight, expansion generated on the animal's left
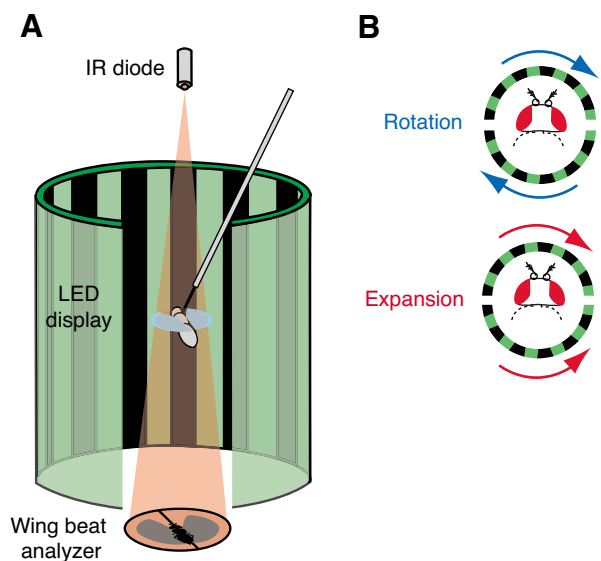

Fig. 1. Experimental apparatus. (A) A digital flight simulator comprises a wrap-around cylinder of light emitting diodes (LED). An infrared (IR) beam casts a shadow of the tethered fly's two wings on an optoelectronic sensor that measures instantaneous changes in right and left wing beat amplitude and frequency in response to image motion. (B) Panoramic patterns of vertical stripes move horizontally to elicit compensatory optomotor steering responses. Visual expansion (bottom) differs from visual rotation (top) only in the direction of motion across the rear field of view.

as well as clockwise rotation resulted in increased ΔWBA, which is tightly correlated with rightward yaw torque. In related experiments, we tested for any influence of side-bias by periodically inverting the direction of visual expansion and rotation. Consistent with many studies of optomotor behavior, we found no significant difference between responses to leftward or rightward motion.

The patterns used here vary as a square-wave of intensity along the azimuth, not sinusoidally. As such, there is significant frequency content above the fundamental spatial frequency defined by the grating period. However, in fruit flies the square-wave does not interfere with the perception of motion responses to the fundamental wavelength. Experiments related to these using similar gratings have revealed that neither the time course nor the magnitude of optomotor flight responses vary between a square-wave pattern and a smooth sinusoidal pattern of the same wavelength (Duistermars et al., 2007). The relative insensitivity to high frequency components of a square-wave

pattern likely reflects the well-known spatial low-pass characteristics of *Drosophila*'s photoreceptor optics as well as the temporal low-pass characteristics of motion processing pathway through the brain, pre-motor pathways and musculoskeletal system.

We first described the spatial and temporal sensitivity of expansion and rotation responses by systematically varying the spatial period of the projected visual pattern and its velocity. The stimulus regime was composed of periods of open-loop large-field expansion or rotation test stimuli interspersed with periods during which the fly had active closed-loop control of a 30° vertical stripe. This stimulus regime insured that flies were actively engaged in optomotor behavior when the test patterns were presented. This was done to insure that each fly was tested under similar optomotor control conditions – in this case fixating a vertical stripe. For all experiments, closed-loop periods lasted 5 s and test periods lasted 3 s each. Test stimuli consisted of a sequence of four increasing velocities repeated for five consecutive spatial period patterns, both for expansion and rotation stimuli. Thus each fly was stimulated with a set of $4 \times 5 \times 2 = 40$ different stimulus conditions – expansion and rotation of five spatial period patterns at four velocities. The spatial patterns were composed of (i) $\lambda^* = 15°$ spatial period with a 75–25%, light:dark duty cycle, (ii) $\lambda = 15°$, 50:50 duty cycle, (iii) $\lambda = 30°$, 50:50 duty cycle, (iv) $\lambda = 60°$, 50:50 duty cycle, (v) $\lambda = 90°$, 50:50 duty cycle. At 50:50 duty cycle, the 15° grating was represented by two ON pixels and two OFF pixels. Thus, for each image displacement, the pattern moved 1/4 wavelength. We therefore included the λ^* grating to control for spatial aliasing. Velocity test values were 10, 169, 232 and 431° s^{-1}. These spatial period and velocity combinations correspond to temporal frequencies ranging from 0.11 Hz to 35.4 Hz. We systematically increased velocity, instead of randomizing them, in order to explicitly test for any significant temporal hysteresis. We found no such effects, probably because the flies had a
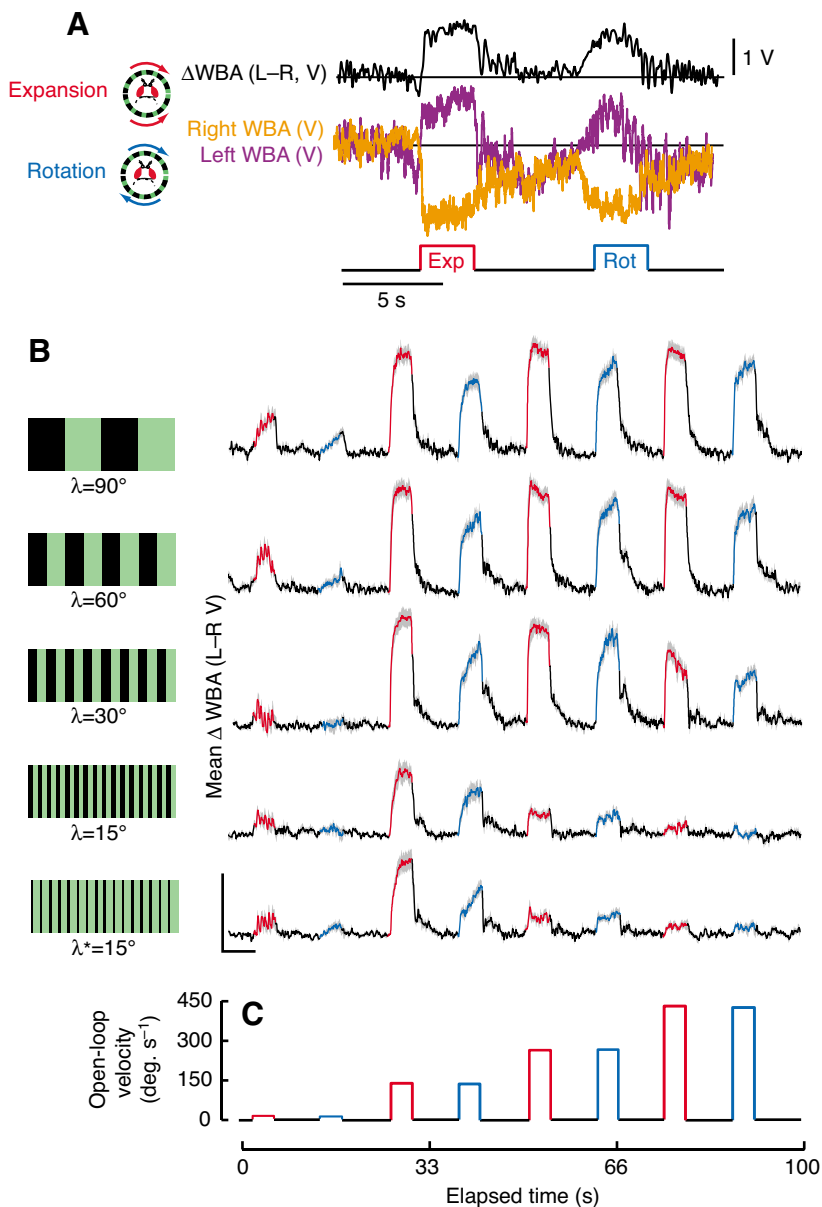

Fig. 2. Optomotor steering responses to panoramic image motion. (A) Example response to a test expansion (Exp) and rotation (Rot) stimulus. In response to expansion from the left, the amplitude of the right wing beat decreases while the amplitude of the left increases. As such left minus right amplitude (ΔWBA) increases in response to both stimuli, but with varying amplitude. Between test periods, the fly has active control of a single vertical stripe. (B,C) Mean responses to systematic variation in the spatial period (B) and velocity of pattern motion (C). Solid line, mean time-averaged responses; gray envelope, s.e.m.; *N*=36 flies. Red segments, 3-s open-loop expansion test periods; blue segments, rotation tests; black segments, intervening 5-s closed-loop control periods. Each row shows mean responses to striped grating spatial period as indicated. ΔWBA, (L–R, V) refers to left minus right wing beat amplitude encoded in V. The time-varying voltage signal is directly proportional to yaw torque.

Table 1. *Two-way repeated measures ANOVA for two within-subjects variables*

ΔWBA source	d.f.	F	P
Vertical extent	15	11	<0.001
Expansion *versus* rotation	1	20	<0.001
Temporal frequency	19	9	<0.001
Expansion *versus* rotation	1	37	<0.001
Unadapted contrast	15	13	<0.001
Expansion *versus* rotation	1	43	<0.001
Adapted contrast	15	11	<0.01
Expansion *versus* rotation	1	22	<0.001

Analyses included expansion *versus* rotation, vertical extent, temporal frequency and two contrast treatments (unadapted and adapted, see Materials and methods). We tested whether ΔWBA responses varied significantly as a result of both the experimental treatment itself (e.g. varying the vertical extent of pattern motion), and the expansion *versus* rotation.

significant duration of closed-loop motion control (roughly 1000 individual wingbeats, roughly the equivalent of 25 free-flight saccades) in between open loop tests to eradicate any influence of time-history.

To map the sensitivity of image contrast for the expansion *versus* rotation stimuli we chose one combination of spatial period and velocity conditions that consistently produced strong optomotor steering responses (λ=30° at 232° s⁻¹). We then constructed expansion and rotation patterns that varied systematically in the intensity of the 'light' and 'dark' parts of the pattern. Contrast, estimated by the Michelson definition as the difference between 'on' and 'off' LED intensity values (I_{max}, I_{min}, respectively) divided by the sum of 'on' and 'off' values [$(I_{max}-I_{min})/(I_{max}+I_{min})$]. We tested optomotor responses to 27 unique contrast values, which were shuffled randomly, and presented in expansion and rotation. We repeated these contrast response experiments under two conditions: contrast unadapted and same-contrast adapted. For the unadapted condition, flies were presented with the stripe under closed-loop control prior to the open-loop test stimulus. As such, there was no prior exposure to the test contrast. To examine the influence of

exposure to the test contrast prior to the test, the usual vertical stripe was replaced with the wide-field test pattern at the selected contrast during the closed-loop period, followed by the open-loop test. Thus, for the same-contrast adapted treatment, there was 7 s of exposure to the test contrast level prior to the test itself.

For each experimental treatment (variation in spatial frequency, temporal frequency and contrast), each fly received the entire series of expansion and rotation stimulus conditions. This design enabled statistical analyses with two-way repeated measures ANOVA for two within-subjects variables (Table 1). Because the different conditions were tested with the same subjects (i.e. within-subject design), statistical significance between the expansion and rotation treatments are not represented by error bars (Masson and Loftus, 2003), which are therefore omitted for clarity.

Time series data including the instantaneous azimuthal position of the visual pattern and stimulus waveform, raw left and right wing stroke amplitude and wingbeat frequency were digitized at 500 Hz (Axon Instruments DigiData 1320, Sunnyvale, CA, USA) and stored on a PC workstation. All analyses were performed using custom software routines written in Matlab (Natick, MA, USA). The raw wingbeat amplitude signals were low-pass filtered at 200 Hz with a 5th order zero-phase digital Butterworth filter. Optomotor responses reach steady state within roughly 1 s, thus for each 3 s test stimulus cycle, we measured the maximum ΔWBA value within the first 1.5 s of the test (roughly 300 wing beats) to quantify response amplitude (R). Data were then normalized to the highest value within each trial (R/R_{max}).

Results

We examined the spatial, temporal and contrast sensitivity of visual motion detection during tethered flight in *Drosophila melanogaster*. During periods of closed-loop control of a single vertical stripe, flies actively balanced the amplitude of the right and left wing beats such that the difference was near zero (Fig. 2A). By contrast, in response to either rotation of the visual panorama, or expansion from one side, stroke amplitude increased on the left side and decreased on the right side (Fig. 2A). Thus, the difference in stroke amplitude increased during test periods corresponding to attempted turns to the right

Fig. 3. Temporal frequency tuning curves for expansion and rotation optomotor responses. Responses to different spatial wavelengths are pooled. Values are means ± s.e.m. for N=36 flies. A Gaussian waveform (to facilitate visual comparison only) is plotted in both panels and is shifted downward ~20% for the rotation plot. Maximum ΔWBA (R/R_{max}) refers to the peak left minus right wingbeat amplitude response (R), divided by the maximum response in the trial (R_{max}).
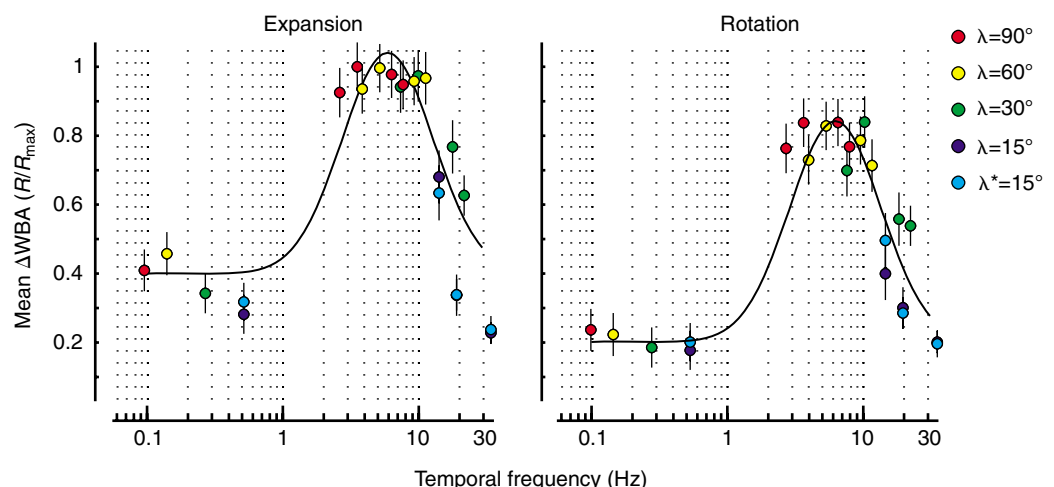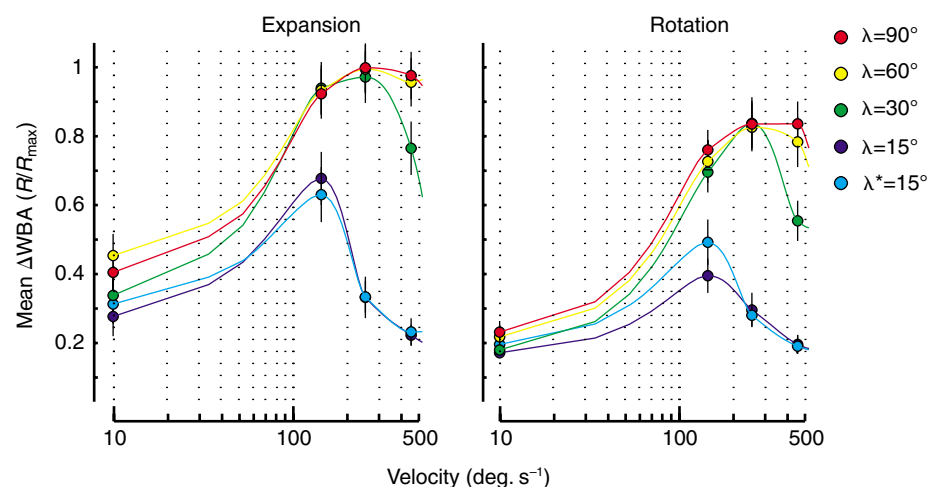
– away from the center of visual expansion (for the expansion stimulus) and following the direction of panoramic visual rotation (for the rotation stimulus). The magnitude and time course of the steering reactions varied according to (1) the temporal frequency of image motion, (2) the spatial period of the display pattern, (3) the periodic contrast and (4) the spatial organization of the stimulus (rotation or expansion). During the test sequences, steering responses to open-loop visual stimuli were robust in that they persisted for the duration of the stimulus, and were also repeatable in that the variance about the mean response trajectory was low (Fig. 2B). On average, low spatial period patterns comprising narrow stripes produced weaker responses by contrast to high spatial period patterns which produced the largest steering responses.

The product of spatial frequency (cycles deg.$^{-1}$, reciprocal of spatial period) and velocity defines the frequency that moving stripes pass over the eye (temporal frequency in cycles s^{-1}). Mean ΔWBA shows a characteristic tuning profile with respect to temporal frequency. For both expansion and rotation stimuli, responses were fairly consistent between 0.1 and 0.6 Hz, then rose steeply to a plateau between 3 and 10 Hz before rolling off at 30 Hz (two-way repeated measures ANOVA $P<0.001$, Table 1). We tested the statistical significance for both the specific treatment (e.g. vertical extent, contrast) and also for the comparison between expansion and rotation. The rotation and expansion stimuli produced similar temporal frequency tuning curves, but rotation responses were attenuated by 20% across the entire range of temporal frequencies (Fig. 3, $P<0.001$ Table 1). To highlight the similarity of temporal tuning between the two visual treatments, we fitted a Gaussian curve (Srinivasan et al., 1999) to the log-transformed expansion data using a least-squares optimization method. We then used the amplitude and position coefficients from the expansion fit and allowed only an offset parameter to be scaled for the rotation data set. R^2 values were similar for both fits (0.82 and 0.89, respectively) with the rotation curve being offset downward on the y-axis by 20% compared to the expansion curve. These results suggest that whereas the gain of optomotor responses is higher for an expansion flow field, the temporal frequency optimum is the same for both expansion and rotation. We pooled the data across spatial wavelengths under the assumption that the optima are similar, but without further experiments we cannot be certain

that this is the case. Nevertheless, even if the optima do vary across spatial wavelength, the variation is qualitatively similar for expansion and rotation (Figs 3, 4), which would support our central claim that spatio-temporal tuning is similar for the two flow fields, whereas response magnitude is generally shifted downward.

Likewise, the spatial frequency sensitivity for expansion and rotation are similar. Mean response values were plotted for each spatial pattern across each test velocity. The data were smoothed with shape-preserving interpolations (Fig. 4). Whereas the plots for the rotation data are shifted downward approximately 20%, there are no conspicuous differences between the spatial tuning profiles for expansion and rotation stimuli; instead the functions peak at the same velocities for each spatial period tested (Fig. 4).

We next explored how optomotor response magnitude is influenced by the vertical extent of pattern motion. This was done by first horizontally 'scanning' the visual field with a 1-pixel row of moving stripes to identify the most sensitive vertical region (Fig. 5A), at which location the pattern was extended vertically in random increments between 1 pixel (3.75°) and 32 pixels (120°). On average, for the 1-pixel row, optomotor steering responses were strongest near the visual equator (Fig. 5B). The mean response trajectories for each of 16 different vertical pattern sizes are color-coded and overlaid in Fig. 5C. These data indicate three things. First, as has been reported previously (Tammero et al., 2004), and indicated in Fig. 2, response trajectory varies strongly between expansion and rotation stimuli. At the onset of constant-velocity motion, expansion responses rise quickly, plateau, then slowly decay, whereas rotation responses rise slowly and instead of decaying continue to rise to the termination of the stimulus. Second, consistent with prior results (Tammero et al., 2004), the pass-band characteristics for stimuli on the frontal and rear visual hemispheres varies markedly. Whereas the frontal stimulus results in a low-pass response trajectory characterized by a rapid onset, syndirectional plateau, and phase-locked decay in the steering reaction during stimulus presentation, motion restricted to the rear hemisphere elicits a response with a lower frequency cut-off (Fig. 5C inset). Third, mean response maxima for the expansion stimulus continue to increase with increasing vertical pattern size (color-coded waveforms in Fig. 5C), but rotation responses are independent of pattern size after the pattern reaches roughly 30° in vertical extent (Fig. 5D). Thus, spatial integration properties, and by implication the underlying neural mechanisms, of expansion-mediated and rotation-mediated optomotor responses are different (Fig. 5D, $P<0.001$ Table 1).

Fig. 4. Tuning curves for spatial wavelength over velocity for expansion and rotation optomotor responses. Data are fitted with shape-preserving interpolant functions (piecewise cubic polynomial) to facilitate visual comparison.
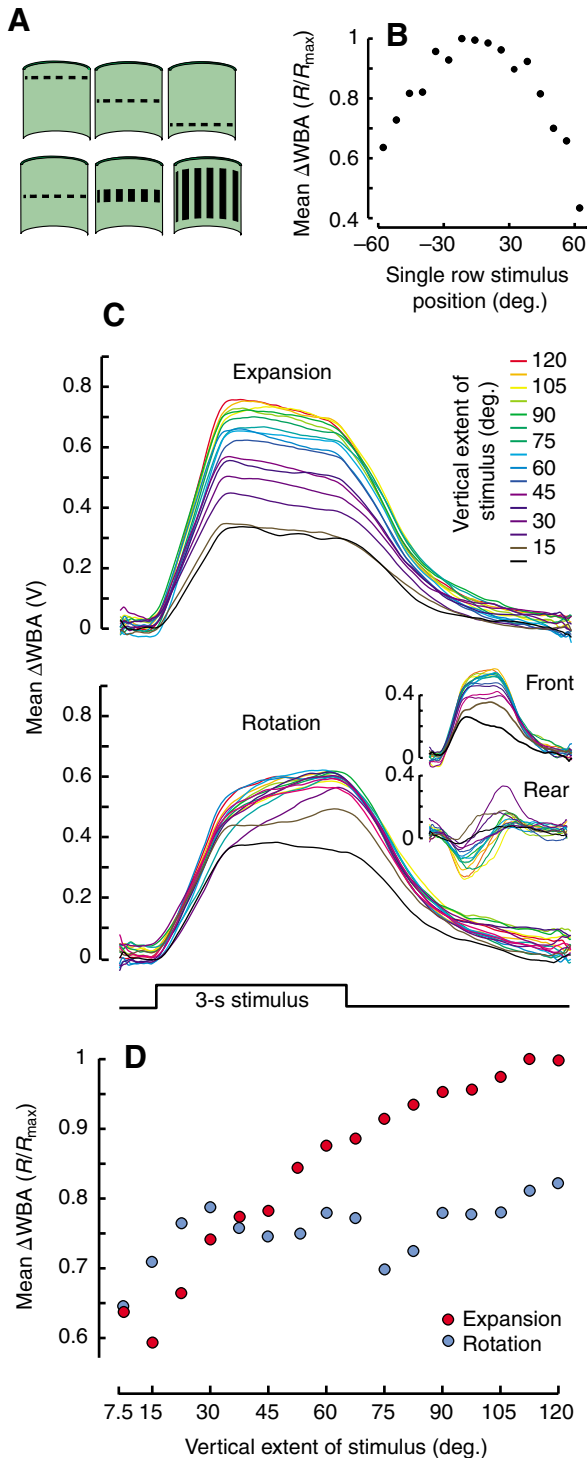
Fig. 5. Optomotor responses vary with the vertical extent of pattern motion. (A) Diagram of visual stimuli. Top row: stimuli used to find the vertical location of the strongest sensitivity to horizontally moving stripe patterns. Bottom row: representations of stimuli that vary in vertical stimulus extent. (B) Response magnitude for a single pixel row of expansion stimuli plotted against the vertical location of the row in the arena, indicating maximum sensitivity in the middle of the arena, where the fly is positioned. (C) Mean response waveforms to visual expansion (top) and visual rotation (bottom) that vary for the vertical extent of image motion (color coded). Insets indicate responses to motion restricted to only the front or rear 180° of the cylindrical arena. (D) Steady-state response amplitude of the waveforms indicated in C for *N*=50 flies.

smooth pattern motion. These results indicate that rotation responses show low-pass characteristics that are largely absent in expansion responses.

Finally, we explored how the periodic contrast of moving patterns differentially influenced optomotor responses to rotation and expansion flow fields. Flies were presented a pattern composed of spatial wavelength λ=30° at a velocity of 232° s^{-1} for 3 s. Pattern contrast ratio varied between 0.008 and 0.93. As discussed above, we ran two experiments: the first was for flies that were tested without any prior exposure to the tested pattern contrast (contrast unadapted) and the second for flies that were presented with the test contrast prior to the test (same-contrast adapted). The results indicate that for both unadapted and adapted conditions, response magnitude varies according to both the contrast and the expansion *versus* rotation structure of visual motion, (two-way repeated measures ANOVA *P*<0.001, Table 1). Expansion consistently elicited larger optomotor responses. For the unadapted flies, low contrast rotation and expansion elicited similar response magnitude (Fig. 7), and as contrast increased expansion responses saturated at 0.3, whereas rotation responses were lower in magnitude, increased monotonically with contrast, and saturated at near 0.93 contrast, 20% lower magnitude than for expansion (Fig. 7, left). For the contrast-adapted flies, the rotation responses were similar to the unadapted condition, but showed slight but insignificant elevated responses across contrasts. Strikingly, the expansion responses showed significantly stronger responses at low contrast (Fig. 7, right).

To quantify the contrast response functions, we fit a sinusoidal function to the data that captures two critical elements of contrast sensitivity – a quadratic dependence at low contrast and response saturation at high contrast:

$$F(x) = \frac{\alpha}{1+e^{[\beta(x-\gamma)]}}.$$

Parameters for the sigmoid function (indicated in Fig. 7) were determined using a Nelder–Mead non-linear optimization algorithm run on the data from each animal. The parameters describe the saturation level (α), the steepness (β) and the rightward shift (γ) of the functions, respectively. For the unadapted rotation function α=0.83, β=–5.6, and γ=–0.1, R^2=0.77. For the unadapted expansion function α=0.95, β=–26 and γ=0.52, R^2=0.85. For adapted rotation α=0.85, β=–5.7 and γ=–0.15, R^2=0.6. For adapted expansion α=0.94, β=–71 and

To further examine the time course of optomotor responses, we stepped the visual stimulus in 3.75° increments at approximately 2 increments s^{-1}. The individual image steps were clearly apparent to a human observer. Each 3.75° image expansion displacement resulted in a rapid turning response phase-locked to the motion cue (Fig. 6). By contrast, the identical stepwise motion of the full-field rotating pattern did not elicit phase-locked torque responses, but rather elicited only a steadily increasing response that is more consistent with

γ=–0.04, R^2=0.13 (note that the low R^2 results from the wing steering responses being independent of contrast due to full saturation). Thus, the rotation response functions saturate at roughly 80% of the expansion response levels, rise roughly 4 times slower with increasing contrast, and are shifted to the right on the contrast axis. Contrast adaptation results in near-immediate saturation of the expansion response function, whereas there is very little change in the rotation function, indicating a strong separation of the two responses at low contrast levels.

Discussion

This central aim of this study was to map the spatial, temporal and contrast sensitivity of optomotor response functions elicited by large-field patterns of visual rotation and side-centered visual expansion in order to examine the hypothesis that the two types of optic flow trigger separate and distinct optomotor response behaviors. Our quantitative behavioral results provide evidence that large-field optomotor expansion and rotation responses are indeed separate responses, which likely serve separate specialized needs of flight control. Our results suggest that the two behaviors are mediated by a common array of elementary motion detectors, but have different spatial integration properties, low-pass characteristics, and contrast sensitivity. This indirectly suggests that the two behaviors are most likely controlled by separate pre-motor motion processing pathways. These conclusions are based on several lines of evidence. The identical spatial and temporal frequency sensitivity optima (Figs 3, 4) suggest that the two flow fields are processed by delay-and-correlate motion detectors containing similar time constants and spatial separation of the input channels. The evidence suggesting that after the elementary detection, the rotation and expansion responses comprise separate control systems comes from three results. First, expansion responses increase linearly with vertical stimulus extent but rotation responses saturate at ~30° (Fig. 5), suggesting distinct spatial integration properties. Second, steering 'spike' responses to intermittent rapid image displacements are conspicuous for an expanding flow field, but not for a rotating one (Fig. 6), suggesting distinct low-pass characteristics. Third, expansion responses persist and are near maximal even under very low contrast conditions, particularly after pre-exposure to the test contrast level (Fig. 7), implying separate contrast sensitivity to expansion and rotation.
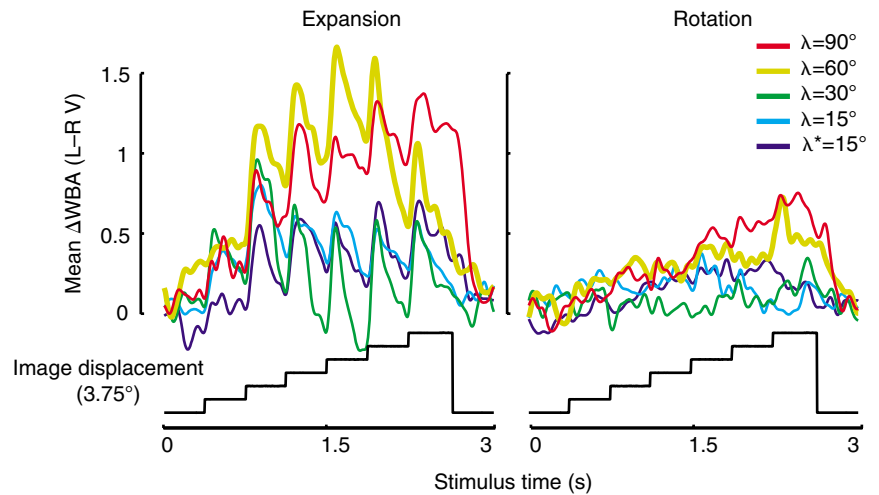

Fig. 6. Mean time course of responses to 1 pixel image displacements (3.75°) at 2 steps s^{-1}. Each waveform represents the mean response for N=36 flies at the color-coded spatial wavelength.
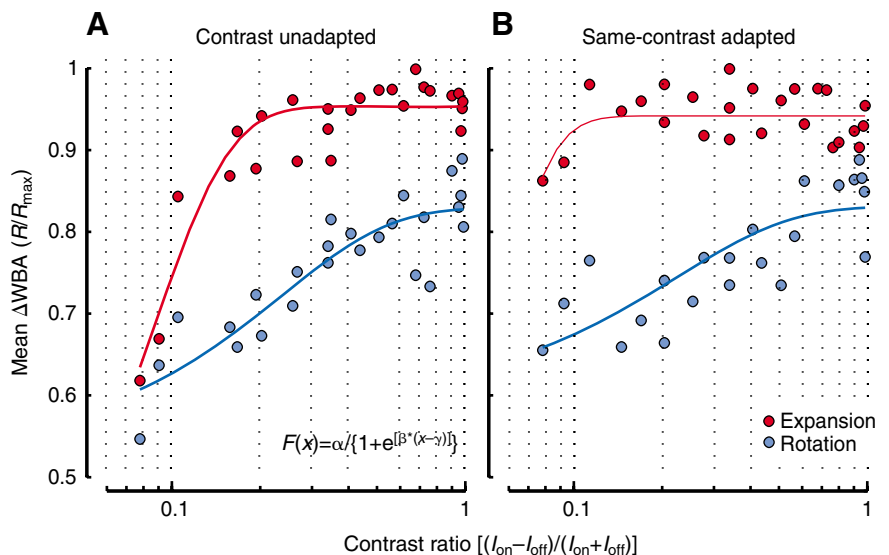

Fig. 7. Optomotor responses vary with image contrast. (A) Mean responses for N=30 flies indicated for an unadapted treatment; flies had no prior exposure to the test stimulus. (B) Mean responses for N=40 flies indicated for a 'same-contrast adapted' treatment; flies were presented with the test pattern contrast for 7 s prior to the open-loop test (see Materials and methods). Data are fit with the sigmoid function indicated. The three function variables were identified with a non-linear least-squares optimization algorithm (see Materials and methods). Within-subject design obviates the need for error bars. Variance across animals was similar to that of Fig. 2.

Relating optomotor behavior to motion detection circuits

Within the earliest stages of motion processing, the apparent direction and strength of image motion is thought to be determined by the spatial separation of visual sampling units such as neighboring ommatidia as well as the delay time constant imposed between two units prior to temporal correlation (Hassenstein and Reichardt, 1956). As such, the magnitude of electrophysiological responses in motion processing neurons as well as yaw torque reactions are bounded

by separable spatial and temporal frequency-sensitivity functions reflecting the properties of the elementary motion detectors (EMDs) (Borst and Egelhaaf, 1993; Egelhaaf and Borst, 1993; Srinivasan et al., 1999). As an abstract model, each EMD is characterized by a unique spatio-temporal frequency function surface. Therefore, optomotor behaviors maximally sensitive to a single spatial wavelength and single temporal frequency very likely draw from a common pool of EMDs. Our results show that the temporal frequency optima for both expansion and rotation optomotor responses lie between 3 and 12 Hz (Fig. 3), and the spatial wavelength sensitivity saturates at $\lambda=30°$. These values are consistent with findings for yaw torque flight optomotor responses in house flies (Borst and Bahde, 1987; Reichardt, 1966) and blow flies (Wehrhahn, 1985), as well as for walking fruit flies (Buchner, 1984), and support the parsimonious hypothesis that the same system of EMDs underlies optomotor responses to both flow fields during flight in fruit flies.

In larger flies, it is thought that input from the retinotopic array of local EMDs and their neuronal correlates is spatially pooled by neurons of the third optic ganglion to construct neural responses to global patterns of optic flow (Higgins et al., 2004; Single and Borst, 1998). Tangential cells of the lobula plate (LPTCs) show spatial integration properties tuned to the orientation and direction of wide-field movement across the retina and play a crucial role in the guidance of optomotor responses (Hausen, 1982; Krapp et al., 1998). Thus, examining how optomotor behavioral responses vary with the extent of motion projected across the retina can be used to estimate the extent of EMD integration and, by extension, the underlying system of LPTCs (Borst and Bahde, 1987). We found that varying the vertical size of the moving pattern had different effects on the expansion and rotation optomotor responses during flight. Whereas rotation responses saturated at roughly 30° pattern size, expansion response amplitude continually increased with increasing pattern size (Fig. 5). These results support the conjecture that the two flow fields are processed by separate ensembles of LPTCs with different, but perhaps overlapping, vertical receptive fields.

The temporal properties of optomotor steering responses to dynamic stimuli have been used to correlate behavior with specific LPTC circuits. House flies (genus Calliphora) show sluggish yaw torque and steering muscle spike modulations in response to panoramic image rotation by comparison to the rapid responses elicited by small object motion (Egelhaaf, 1987; Egelhaaf, 1989). These behavioral responses correlate tightly with the membrane responses of wide-field horizontal system cells (HS) and small-field feature detection cells (FD) of the lobular plate (Egelhaaf et al., 1988), implying that HS participates in relatively slow wide-field optomotor reflexes, whereas FD participates in object tracking or body saccades with a much shorter time constant. Here, we show that intermittent displacement steps of a laterally expanding image results in rapid high-amplitude torque responses, whereas a rotating image produces only gradual syndirectional shifts in the steering signal, but without rapid fluctuations (Fig. 6). We take this as evidence that the expansion optomotor response is low-pass filtered with a shorter time constant than the rotation response, owing to separate pre-motor motion processing

pathways with different temporal dynamic properties. One important caveat: we know little of motion processing in *Drosophila*, but the horizontal and vertical system cells show similar anatomical architecture, with perhaps fewer wide-field cells (Scott et al., 2002).

In addition to the spatial and temporal frequency characteristics, the detection of visual motion depends upon the periodic contrast of moving images. The sensitivity to image contrast of either simulated EMDs, LPTC recordings or behaving flies is non-linear such that at a given spatial wavelength, response amplitude shows a quadratic dependence at low contrast and saturates at higher contrast levels (Buchner, 1984; Dvorak et al., 1980; Harris et al., 2000). Flight optomotor responses also show a saturated-quadratic functional dependence of image contrast (Dvorak et al., 1980), but the shape of the response functions differ in that expansion sensitivity saturates at a higher value, shows a steeper rise, and is shifted rightward on the contrast axis by comparison to rotation (Fig. 7). Do these different parameters suggest separate underlying pathways? Individual LPTC neurons (HS) display motion adaptation that effectively shifts the sensitivity curve rightward on the contrast axis, but does not alter the shape of the response function (Harris et al., 2000). Thus, it is certainly possible that the rotation saturation level is 'clipped' by a rightward shift in contrast sensitivity within a single neuronal circuit responding with higher gain to expansion than rotation, but that does not account for the further change in the shape of the two curves. Nevertheless, a stronger separation between the expansion and rotation responses to image contrast emerges after flies are exposed to the stimulus contrast pattern for some time prior to the actual open-loop test. We refer to this treatment as 'same-contrast adaptation', and it results in a strong increase in contrast sensitivity (particularly to low contrast) within expansion responses but no significant change in rotation responses (Fig. 7). Contrast dependence of visual motion detection has been attributed to the saturation nonlinearities prior to or within the EMDs (Egelhaaf and Borst, 1989), and may minimize the dependency on specific contrast by LPTCs (Dror et al., 2001). Yet, we are suggesting here that the two control systems have common local movement detectors, so where does the variation in contrast sensitivity for rotation and expansion optomotor behaviors come from? The simplest hypothesis is that the behavioral contrast sensitivity is layered upon the control systems by circuits postsynaptic to the LPTCs. For example, pre-motor descending interneurons for the two optomotor responses may pool from LPTCs with varying EMD input and explicit contrast sensitivity. Nevertheless, at the very least, these results suggest that the sensitivity to image contrast is qualitatively different for responses to large-field patterns of rotation and expansion, which can be parsimoniously explained by the presence of two parallel pre-motor large-field expansion and rotation circuits with different intrinsic sensitivity to image contrast.

What are the possible parallel visual circuits for expansion and rotation selectivity? Whereas the reconstructed receptive fields of some LPTCs appear to be matched for spatially complex panoramic optic flow patterns generated by flight maneuvers such as pitch and roll (Krapp, 2000; Krapp and Hengstenberg, 1996), there are as yet no reports of LPTCs that specifically encode either patterns of image expansion centered laterally. The equatorial horizontal system cell (HSE), once

thought to encode panoramic rotation, fails to do sounder naturalistic optic flow conditions (Kern et al., 2001). Since LPTCs show extensive heterolateral connections (Haag and Borst, 2002), it seems reasonable that complex optic flow patterns are encoded by groups of LPTCs with distinct but overlapping receptive fields. Postsynaptic to the LPTCs, pre-motor descending visual interneurons may assemble spatially sensitivity for expansion and rotation, and convey this information to relevant steering and power muscle motor networks. Whereas it is certainly the most studied visual neuropile in the fly, the lobula plate is by no means the only place where motion circuits reside. Expansion-sensitive interneurons have been reported within the optic lobes and midbrain in locusts (Gabbiani et al., 1999; Judge and Rind, 1997), mantids (Kral and Prete, 2004), and hawkmoths (Wicklein and Strausfeld, 2000). Finally, it is at least conceivable that the two optomotor behaviors reflect two systems of EMDs having different directional sensitivities converging onto a common pre-motor descending pathway. This scenario would suggest that the differences in response dynamics must emerge entirely from the EMDs, which is not likely. Whatever the underlying visual circuit – as yet undisclosed – it would appear that large-field rotation and expansion mediated optomotor responses are indeed separate and distinct behaviors, serving different roles for flight control, and coordinated by separate parallel pathways.

Advantages of separate rotation and expansion control systems

Maintaining dynamic optomotor equilibrium, avoiding approaching obstacles or tracking visual objects, require encoding these environmental features correctly. Separate neural circuits dedicated to expansion and rotation stimuli ensure response specificity under different sensory conditions. For example, the high-gain expansion circuit may mediate rapid collision avoidance and escape from approaching predators, whereas the rotation circuit may mediate stability during slow flight or hovering. Consistent with the steady-state optomotor responses described here, under dynamic stimulus conditions large-field expansion generates larger steering responses than rotation at a wide range of motion frequencies, suggesting that the expansion response generally operates at higher gain than rotation responses (Duistermars et al., 2007).

There is some corroborating free-flight behavioral evidence for the operation of two distinct control systems. During free flight, fruit flies execute segments of straight flight interspersed with rapid 90° turns called saccades (Tammero and Dickinson, 2002a). Saccadic motor patterns are used by animals as diverse as humans (Land, 1992) and house flies (Schilstra and van Hateren, 1998) to minimize the corrupting influence of motion blur and maintain stable gaze. During free flight, *Drosophila* saccades are threshold-triggered by a monotonic increase in the magnitude of contralateral large-field retinal expansion, but not rotation (Tammero and Dickinson, 2002a). However, between ballistic expansion-elicited saccades, the flight path is not exactly straight but rather is slightly curved depending on the proximity of the nearest wall (although the direction of the curved turn is away from the closest wall, not toward it, so the turn cannot be explained by a purely syndirectional rotational optomotor reflex). Curved flight paths are readily observed

within visual environments composed of high contrast horizontal stripe, which generate strong vertical motion cues without strong horizontal motion cues (Frye and Dickinson, 2007). Recent evidence from blow flies suggests that it is during these inter-saccade flight segments that the visual system encodes the spatial layout of the visual environment (Kern et al., 2005).

Expansion responses themselves mediate several important behaviors during flight. Results obtained with tethered *Drosophila* show that visual processing is likely further segregated into parallel collision avoidance and landing behaviors. A laterally expanding object elicits rapid and robust steering responses oriented away from the focus of expansion. By contrast, the same stimulus presented within the frontal field of view elicits a leg kick, without a steering response, thought to comprise an attempt to land. Both the spatial and temporal properties of these two reflexes strongly implicate the operation of parallel underlying circuits (Tammero and Dickinson, 2002b). Theoretical analyses have suggested that visual expansion selectivity can provide an unambiguous cue to dynamically maintain an upwind flight posture (Reiser et al., 2004). Electrophysiological recordings from the cervical connective in blowflies have revealed a group of expansion-sensitive descending pre-motor interneurons that likely mediate landing responses (Borst, 1990). There are scant physiological analyses of identified descending neurons in flies [but see Gronenberg and Strausfeld (Gronenberg and Strausfeld, 1992) for small object selective cells]. The evidence presented here motivates the hypothesis that descending pathways may draw from lobula plate cell systems with distinct by overlapping receptive fields in order to multiplex expansion and rotation sensitive signals for the flight motor circuits of the thorax. For simplicity, we have discussed LPTC architecture as if it were common to fruit flies and their larger cousins. Do fruit flies and house flies or blow flies have similar optomotor control circuits? As yet, we simply do not know; whereas structural and developmental evidence supports the notion of functional analogy (Scott et al., 2002; Scott et al., 2003), there is as yet no direct physiological evidence to suggest similar LPTC function. Furthermore, by contrast to well-studied blow flies and house flies, fruit flies hover, which may place unique demands on the visual system in these animals. It will be interesting to reveal the neural specializations for expansion and rotation optomotor responses, as well as to match these behavioral control circuits to the comparative sensory ecology flight control in different insect species.

List of abbreviations

ΔWBA	left plus right (difference) wing beat amplitude
ΣWBA	left plus right (sum) wing beat amplitude
LPTC	lobula plate tangential cell
EMD	elementary motion detector
HS	horizontal system of the lobular plate
FD	feature detection cells of the lobular plate
HSE	horizontal system equatorial cell

References

Borst, A. (1990). How do flies land? From behavior to neuronal circuits. *Bioscience* **40**, 292-299.

Borst, A. and Bahde, S. (1987). Comparison between the movement detection systems underlying the optomotor and the landing response in the housefly. *Biol. Cybern.* **56**, 217-224.

Borst, A. and Egelhaaf, M. (1993). Detecting visual motion, theory and models. In *Visual Motion and its Role in the Stabilization of Gaze* (ed. F. A. Miles and J. Wallman), pp. 3-27. New York: Elsevier Science Publishers.

Buchner, E. (1984). Behavioral analysis of spatial vision in insects. In *Photoreception and Vision in Invertebrates* (ed. M. Ali), pp. 561-522. New York: Plenum.

Collett, T. S. (1980). Some operating rules for the optomotor system of a hoverfly during voluntary flight. *J. Comp. Physiol. A* **138**, 271-282.

Dahmen, H.-J., Franz, M. O. and Krapp, H. G. (2001). Extracting egomotion from optic flow: limits and accuracy of neural matched filters. In *Motion Vision* (ed. J. M. Zanker and J. Zeil), pp. 143-168. Berlin, Heidelberg, New York: Springer-Verlag.

Dickinson, M., Lehman, F. and Chan, W. (1998). The control of mechanical power in insect flight. *Am. Zool.* **38**, 718-728.

Duistermars, B. J., Reiser, M. B., Zhu, Y. and Frye, M. A. (2007). Dynamic properties of large-field and small-field optomotor flight responses in *Drosophila*. *J. Comp. Physiol. A* **193**, 787-799.

Dror, R. O., O'Carroll, D. C. and Laughlin, S. B. (2001). Accuracy of velocity estimation by Reichardt correlators. *J. Opt. Soc. Am.* **18**, 241-252.

Dvorak, D., Srinivasan, M. V. and French, A. S. (1980). The contrast sensitivity of fly movement-detecting neurons. *Vision Res.* **20**, 397-407.

Egelhaaf, M. (1987). Dynamic properties of two control-systems underlying visually guided turning in houseflies. *J. Comp. Physiol. A* **161**, 777-783.

Egelhaaf, M. (1989). Visual afferences to flight steering muscles controlling optomotor responses of the fly. *J. Comp. Physiol. A* **165**, 719-730.

Egelhaaf, M. and Borst, A. (1989). Transient and steady-state response properties of movement detectors. *J. Opt. Soc. Am.* **6**, 116-127.

Egelhaaf, M. and Borst, A. (1993). Movement detection in arthropods. *Rev. Oculomot. Res.* **5**, 53-77.

Egelhaaf, M., Hausen, K., Reichardt, W. and Wehrhahn, C. (1988). Visual course control in flies relies on neuronal computation of object and background motion. *Trends Neurosci.* **11**, 351-358.

Frye, M. A. and Dickinson, M. H. (2007). Visual edge orientation shapes free-flight behavior in *Drosophila*. *Fly* **1**, e1-e2.

Gabbiani, F., Krapp, H. G. and Laurent, G. (1999). Computation of object approach by a wide-field, motion-sensitive neuron. *J. Neurosci.* **19**, 1122-1141.

Götz, K. G. (1964). Optomotor studies of the visual system of several eye mutants of the fruit fly *Drosophila*. *Kybernetik* **2**, 77-92.

Götz, K. G. (1975). The optomotor equilibrium of the *Drosophila* navigation system. *J. Comp. Physiol. A* **99**, 187-210.

Götz, K. G. (1987). Course-control, metabolism and wing interference during ultralong tethered flight in *Drosophila melanogaster*. *J. Exp. Biol.* **128**, 35-46.

Götz, K. and Wandel, U. (1984). Optomotor control of the force of flight in *Drosophila* and *Musca*. II. Covariance of list and thrust in still air. *Biol. Cybern.* **51**, 135-139.

Gronenberg, W. and Strausfeld, N. J. (1992). Premotor descending neurons responding selectively to local visual-stimuli in flies. *J. Comp. Neurol.* **316**, 87-103.

Haag, J. and Borst, A. (2002). Dendro-dendritic interactions between motion-sensitive large-field neurons in the fly. *J. Neurosci.* **22**, 3227-3233.

Harris, R. A., O'Carroll, D. C. and Laughlin, S. B. (2000). Contrast gain reduction in fly motion adaptation. *Neuron* **28**, 595-606.

Hassenstein, B. and Reichardt, W. (1956). Systemtheoretische analyse der zeit-, Reihenfolgen- und vorzeichenauswertung bei der bewegungsperzeption des russelkafers *Cholorophanus*. *Z. Naturforsch. B* **11**, 513-524.

Hausen, K. (1982). Motion sensitive interneurons in the optomotor system of the fly. II. The horizontal cells: receptive-field organization and response characteristics. *Biol. Cybern.* **46**, 67-79.

Heisenberg, M. and Wolf, R. (1984). *Vision in Drosophila*. Berlin: Springer-Verlag.

Higgins, C. M., Douglass, J. K. and Strausfeld, N. J. (2004). The computational basis of an identified neuronal circuit for elementary motion detection in dipterous insects. *Vis. Neurosci.* **21**, 567-586.

Judge, S. J. and Rind, F. C. (1997). The locust DCMD, a movement-detecting neurone tightly tuned to collison trajectories. *J. Exp. Biol.* **200**, 2209-2216.

Kern, R., Petereit, C. and Egelhaaf, M. (2001). Neural processing of naturalistic optic flow. *J. Neurosci.* **21**, 1-5.

Kern, R., van Hateren, J. H., Michaelis, C., Lindemann, J. P. and Egelhaaf, M. (2005). Function of a fly motion-sensitive neuron matches eye movements during free flight. *PLoS Biol.* **3**, 1130-1138.

Kral, K. and Prete, F. (2004). In the mind of a hunter: the visual world of the praying mantis. In *Complex Worlds from Simpler Nervous Systems* (ed. F. Prete), pp. 75-115. Cambridge: The MIT Press.

Krapp, H. G. (2000). Neuronal matched filters for optic flow processing in flying insects. *Int. Rev. Neurobiol.* **44**, 93-120.

Krapp, H. G. and Hengstenberg, R. (1996). Estimation of self-motion by optic flow processing in single visual interneurons. *Nature* **384**, 463-466.

Krapp, H. G., Hengstenberg, B. and Hengstenberg, R. (1998). Dendritic structure and receptive-field organization of optic flow processing interneurons in the fly. *J. Neurophysiol.* **79**, 1902-1917.

Land, M. F. (1992). Visual tracking and pursuit: humans and arthropods compared. *J. Insect Physiol.* **38**, 939-951.

Masson, M. E. J. and Loftus, G. R. (2003). Using confidence intervals for graphically based data interpretation. *Can. J. Exp. Psychol.* **57**, 203-220.

O'Carroll, D. C., Bidwell, N. J., Laughlin, S. B. and Warrant, E. J. (1996). Insect motion detectors matched to visual ecology. *Nature* **382**, 63-66.

Reichardt, W. (1966). Detection of single quanta by the compund eye of the fly Musca. In *Proceedings of the International Symposium on the Functional Organization of the Compound Eye* (ed. C. G. Bernhard), pp. 267-289. Oxford: Pergamon Press.

Reiser, M. B. and Dickinson, M. H. (2007). A modular display system for insect behavioral neuroscience. *J. Neurosci. Meth.* In press.

Reiser, M. B., Humbert, J. S., Dunlop, M. J., Del Vecchio, D., Murray, R. M. and Dickinson, M. H. (2004). Vision as a compensatory mechanism for disturbance rejection in upwind flight. In *Proceedings of the American Control Conference*. Vol. 1, pp. 311-316. www.ieeexplore.ieee.org.

Sandini, G., Panerai, F. and Miles, F. A. (2001). The role of inertial and visual mechanisms in the stabilization of gaze in natural and artificial systems. In *Motion Vision* (ed. J. M. Zanker and J. Zeil), pp. 190-214. Berlin, Heidelberg, New York: Springer-Verlag.

Schilstra, C. and van Hateren, J. H. (1998). Stabilizing gaze in flying blowflies. *Nature* **395**, 654.

Scott, E. K., Raabe, T. and Luo, L. (2002). Structure of the vertical and horizontal system neurons of the lobula plate in *Drosophila*. *J. Comp. Neurol.* **454**, 470-481.

Scott, E. K., Reuter, J. E. and Luo, L. (2003). Dendritic development of *Drosophila* high order visual system neurons is independent of sensory experience. *BMC Neurosci.* **4**, 1-6.

Single, S. and Borst, A. (1998). Dendritic integration and its role in computing image velocity. *Science* **281**, 1848-1850.

Srinivasan, M. V., Poteser, M. and Kral, K. (1999). Motion detection in insect orientation and navigation. *Vision Res.* **39**, 2749-2766.

Tammero, L. F. and Dickinson, M. H. (2002a). The influence of visual landscape on the free flight behavior of the fruit fly *Drosophila melanogaster*. *J. Exp. Biol.* **205**, 327-343.

Tammero, L. F. and Dickinson, M. H. (2002b). Collision-avoidance and landing responses are mediated by separate pathways in the fruit fly, *Drosophila melanogaster*. *J. Exp. Biol.* **205**, 2785-2798.

Tammero, L. F., Frye, M. A. and Dickinson, M. H. (2004). Spatial organization of visuomotor reflexes in *Drosophila*. *J. Exp. Biol.* **207**, 113-122.

Wehrhahn, C. (1985). Visual guidance of flies during flight. In *Comprehensive Insect Physiology, Biochemistry, and Pharmacology* (ed. G. A. Kerkut and L. I. Gilbert), pp. 673-684. Oxford: Pergamon Press.

Wicklein, M. and Strausfeld, N. J. (2000). Organization and significance of neurons that detect change of visual depth in the hawk moth *Manduca sexta*. *J. Comp. Neurol.* **424**, 356-376.

Zanker, J. M. and Zeil, J. (2001). *Motion Vision*. Berlin, Heidelberg, New York: Springer-Verlag.